

## Transitional dissipative mechanisms in the fission-like fragmentation of medium-mass nuclear systems

P. Boccaccio, L. Vannucci, and M. Bettiolo

*Istituto Nazionale di Fisica Nucleare, Laboratori Nazionali di Legnaro, Padova, Italia*

L. Lavagnini and G. Vannini

*Istituto Nazionale di Fisica Nucleare, Sezione di Bologna, Italy  
and Dipartimento di Fisica dell'Università, Trieste, Italy*

I. Massa

*Istituto Nazionale di Fisica Nucleare, Sezione di Cagliari, Italy  
and Dipartimento di Fisica dell'Università, Cagliari, Italy*

R. A. Ricci

*Istituto Nazionale di Fisica Nucleare, Laboratori Nazionali di Legnaro, Padova, Italia  
and Dipartimento di Fisica dell'Università, Padova, Italia*

I. Iori

*Istituto Nazionale di Fisica Nucleare, Sezione di Milano, Italia  
and Dipartimento di Fisica dell'Università, Milano, Italia*

G. Guillaume, J. P. Coffin, P. Fintz, and F. Rami

*Centre de Recherches Nucleaires et Université Louis Pasteur, Strasbourg, France  
(Received 15 March 1988)*

Transitional dissipative mechanisms in the fissionlike decay of medium mass composite systems have been studied systematically. Fragments produced in the collision of 4–7 MeV/nucleon,  $A = 19$ –37 projectiles, with  $A = 59$ –89 target nuclei, were identified by time-of-flight spectrometers. Mass, energy, and angular distributions of the fissionlike fragments have been reproduced by dynamical model calculations based on the transport theory. Systematics of lifetimes of the intermediate complex systems are given, indicating a clear dependence on the bombarding energy and entrance channel mass asymmetry.

### I. INTRODUCTION

The study of heavy-ion collisions at bombarding energies  $E/A \lesssim 10$  MeV/nucleon has shown the existence of two dissipative mechanisms, i.e., fusion and deep inelastic collisions (DIC). An early interpretation of the observed phenomena in terms of these competing mechanisms, was based on a schematic picture of the collision process. Depending on the topology of the entrance channel potential, either attractive forces, leading to a mononucleus, or repulsive forces, leading to a dinucleus, were considered to determine the reaction path. However, further experimental results indicated the existence of intermediate regimes (the “fast fission” and “quasifission” processes), which suggested that not only the entrance channel potential, but the overall dynamics of the collision process had to be considered. Actually, in the recent “fast-fission”<sup>1</sup> and “extra-push”<sup>2</sup> models, the collision dynamics is considered explicitly along the whole reaction path, through the multidimensional space of the relevant collective degrees of freedom of the nuclear system. On the other hand, different approaches to a dynamical descrip-

tion of dissipative collisions, based on quantum-statistical theories, have been successfully employed in reproducing experimental data obtained from the study of DIC. In this respect, a recent and refined version of the transport theory<sup>3</sup> has stressed the role of angular momentum in the diffusive relaxation of a dinuclear system by statistical nucleon exchange between the interacting nuclei.

Experimental evidence of transitional dissipative mechanisms in the medium mass ( $A \approx 100$ ) region has been found in several studies at the Strasbourg and the Legnaro Tandem facilities.<sup>4–6</sup> The fissionlike fragmentation of composite systems formed at incident energies around 4–7 MeV/nucleon exhibits certain peculiar characteristics which cannot be understood in terms of pure DIC or fusion processes. Furthermore, such intermediate mechanisms cannot be described in the framework of “fast-fission” or “extra-push” models, because the necessary conditions for their validity (vanishing fission barrier due to large angular momenta and large fissility, respectively) are generally not fulfilled in this mass region.<sup>7</sup> The observed features were explained in terms of a continuous relaxation process, leading the composite system from the

entrance channel to more or less equilibrated configurations, depending on the system lifetime.<sup>6</sup>

With the aim of attaining a more complete understanding of these phenomena, we report in this work the results of a systematic investigation on the characteristics of transitional dissipative mechanisms in the medium-mass region. To study the dependence of the reaction mechanism on the entrance channel mass asymmetry, different projectile-target combinations were chosen to form a given  $(Z_{CS}, A_{CS})$  composite system. In these reactions, in order to have comparable experimental conditions, the incident energies were chosen in such a way that the grazing and the critical angular momenta were similar for all combinations producing the same composite system. Furthermore, other reactions were used to investigate the dependence of the reaction mechanism on the total mass of the composite system, which can be of importance as suggested in an earlier study by Oeschler *et al.*<sup>9</sup> To this purpose, the incident energies were selected to obtain comparable values of the center-of-mass (c.m.) energy of Coulomb barrier ratios. Systematics of lifetimes, obtained from data analysis by a dynamical model,<sup>6,8</sup> will be presented. The dependence of lifetime on the composite system and the entrance-channel configuration is investigated, with particular emphasis on possible correlations with the composite system mass and the entrance-channel mass asymmetry. The resulting fundamental role of the mass asymmetry in the reaction mechanism is underlined and discussed.

The experimental procedure is described in Sec. II, results are presented in Sec. III, data analysis and discussion in Sec. IV, and, finally, conclusions are drawn in Sec. V.

## II. EXPERIMENTAL METHOD

### A. General considerations

To investigate the transitional mechanisms in medium-mass nuclear systems, ten reactions leading to six different composite systems have been studied. The aim of these measurements was to observe the behavior of fissionlike processes as a function of both the entrance-channel mass asymmetry and the composite system mass ( $A_{CS}$ ).

Attention was focused on heavy fragments ( $A > A_{CS}/2$ ), since their observation at forward angles is related to a particular experimental condition which selects events corresponding to the decay of long-lived composite systems (i.e., those surviving for at least half a rotation). In the case of a small mass transfer between the interacting nuclei, this condition can be simply illustrated as in Fig. 1. It is seen that, depending on the interaction time  $\Delta t$  (i.e., the time interval over which nuclear forces are effective), the emission angle for the heavy fragment,  $\theta_e^H$ , varies from a backward angle ( $2\pi - \theta_{gr}^H$ , for  $\Delta t \approx 0$ ) to a forward angle (for longer  $\Delta t$ ), according to

$$\Delta\theta = \omega\Delta t = \pi + \theta_{gr}^L - \theta_e^H, \quad (1)$$

where  $\Delta\theta$  is the rotation angle,  $\omega$  the ( $l$  averaged) angular velocity,  $\theta_{gr}^L$  and  $\theta_{gr}^H$  the grazing angles for the projectile-

like and targetlike fragments, respectively, so that  $\theta_{gr}^L + \theta_{gr}^H = \pi$ . By similar considerations, in the case of projectilelike fragments emitted at  $\theta_e^L \leq \theta_{gr}^L$ , the above relationship reads  $\Delta\theta = \theta_{gr}^L - \theta_e^L$ . The use of these formulas to estimate the interaction times for the emission of projectilelike and targetlike fragments at  $\theta_L = 10^\circ$  from the  $^{32}\text{S} + ^{59}\text{Co}$  reaction at 5 MeV/nucleon incident energy yields  $\Delta t \approx 3 \times 10^{-22}$  s and  $2 \times 10^{-21}$  s, respectively.

In Table I the projectile-target combinations studied in the present work are listed, together with some relevant information on the composite systems. In particular, the entrance-channel mass asymmetry,  $y = (A_t - A_p)/(A_t + A_p)$ , the compound-nucleus fissility<sup>10</sup>

$$x = \frac{Z_{CS}^2 / A_{CS}}{50.88 \{1 - 1.7826[(N_{CS} - Z_{CS}) / A_{CS}]^2\}}, \quad (2)$$

and the c.m. energy to Coulomb barrier ratio,  $E_{c.m.}/B_C$ . Measurements corresponding to the lower range of incident energies ( $E/A < 5$  MeV/nucleon) have been generally performed at the Legnaro Tandem facility, while for the higher energy measurements the Strasbourg Tandem accelerator was employed. Some of the reactions reported in Table I were studied previously and the results are published in the listed references.

### B. Experimental details

The experimental setup, described in more detail in Refs. 4 and 6 consisted of time-of-flight (TOF) telescopes employing microchannel plate start detectors and silicon surface-barrier stop detectors. Additional silicon surface-barrier detectors were placed at forward angles for beam monitoring and normalization purposes. Coincidence TOF energy measurements were performed at

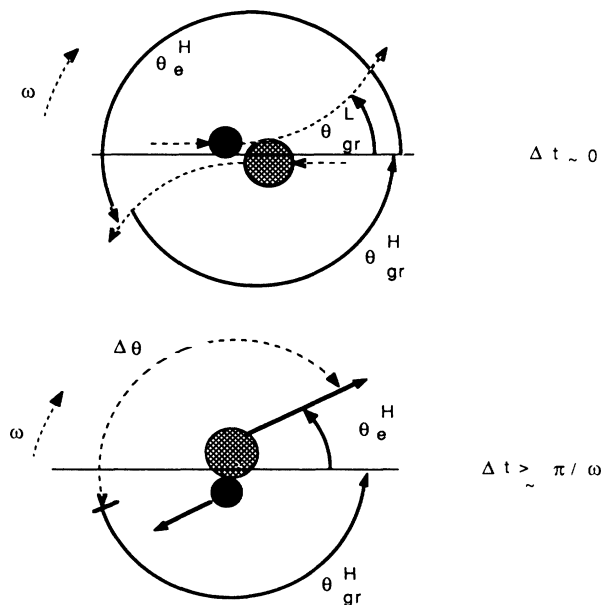


FIG. 1. Center-of-mass scattering geometry for a dissipative collision.

TABLE I. List of the reactions studied in the present work with relevant parameters: the entrance-channel mass asymmetry ( $y$ ), the compound-nucleus fissility ( $x$ ), the c.m. energy to Coulomb barrier ratio ( $E_{c.m.}/B$ ).  $E_i$  is the laboratory incident energy.

Reaction	CN	$y$	$x$	$E_i$ (MeV)	$E_{c.m.}/B$	Ref.
$^{32}\text{S} + ^{59}\text{Co}$	$^{91}\text{Tc}$	0.30	0.40	126,140,154,168	1.5-2.0	6
$^{28}\text{Si} + ^{63}\text{Cu}$	$^{91}\text{Tc}$	0.38	0.40	128,143,158,178,198	1.5-2.3	5
$^{32}\text{S} + ^{63}\text{Cu}$	$^{95}\text{Rh}$	0.33	0.42	134,148,158,169,190	1.8-2.5	<sup>a</sup>
$^{32}\text{S} + ^{63}\text{Cu}$	$^{95}\text{Rh}$	0.33	0.42	126,140,154,168	1.4-1.9	6
$^{35}\text{Cl} + ^{65}\text{Cu}$	$^{100}\text{Pd}$	0.30	0.42	200	2.1	<sup>a</sup>
$^{37}\text{Cl} + ^{65}\text{Cu}$	$^{102}\text{Pd}$	0.27	0.41	145,185	1.5-1.9	<sup>a</sup>
$^{28}\text{Si} + ^{74}\text{Ge}$	$^{102}\text{Pd}$	0.45	0.41	137,151,170	1.7-2.2	<sup>a</sup>
$^{32}\text{S} + ^{76}\text{Ge}$	$^{108}\text{Cd}$	0.41	0.43	158,178,198,218,225	1.7-2.5	4
$^{19}\text{F} + ^{89}\text{Y}$	$^{108}\text{Cd}$	0.65	0.43	155	2.9	<sup>a</sup>
$^{32}\text{S} + ^{85}\text{Rb}$	$^{117}\text{I}$	0.45	0.48	170	1.7	9
$^{28}\text{Si} + ^{89}\text{Y}$	$^{117}\text{I}$	0.52	0.48	148,161	1.6-1.8	<sup>a</sup>

<sup>a</sup>Present work.

observation angles within the  $\theta_L = 5^\circ - 40^\circ$  range. The TOF time resolution ( $\Delta T \approx 200$  ps FWHM) and energy resolution ( $\Delta E/E < 1\%$ ) for fissionlike events allowed the fragment masses to be measured with a resolution  $\Delta A/A \approx \frac{1}{80}$ . Target thicknesses were typically  $\approx 100$   $\mu\text{g}/\text{cm}^2$ . Absolute cross sections were obtained by means of a normalization procedure, which exploited the elastic scattering data measured by the TOF telescope and the monitors. This procedure is estimated to introduce a scale uncertainty in the absolute cross sections of about 10%. The fragment production cross sections were evaluated in the c.m. system by transporting the events of energy-mass scatter plots from the laboratory to the c.m. Data are presented in mass bins of 3 to 4 amu in order to have statistical errors generally not larger than 10%. As explained in Refs. 4 and 6, data were corrected for angular straggling effects, telescope detection efficiency, and light particle evaporation. These corrections were generally small (less than 5%), and the corresponding errors negligible. As the present analysis is focused on fragments having masses  $A > A_{CS}/2$ , the events under consideration are not contaminated by products of reactions induced by the beam on carbon target backings or on light target contaminants.

### III. RESULTS

The class of fissionlike events under study is seen to lie on a locus in the mass-energy plot (see, e.g., Fig. 2) corresponding to the Coulomb repulsion of two charged spheres. For all the incident energies and observation angles of the present measurements, the fragment kinetic energies are found to correspond to a two-body  $Q$  value ranging between  $-20$  and  $-70$  MeV. Selection of data within this  $Q$ -value range, in addition to two-body kinematic constraints, allows discrimination against the bulk of the evaporation residue events.

#### A. Mean total kinetic energies of the fissionlike fragments

Previous coincidence measurements of fissionlike products from the  $^{32}\text{S} + ^{50}\text{Ti}$  (Ref. 11) and  $^{32}\text{S} + ^{59}\text{Co}$  (Ref. 5)

reactions have shown the binary nature of the fragmentation process in the medium-mass region at incident energies in the MeV/nucleon range. Under this assumption, the mean total kinetic energies (TKE) of the fissionlike events in the present study were evaluated in the c.m. using two-body kinematics. Selected TKE distributions, as a function of fragment mass, are presented in Figs. 3 and 4 for the  $^{28}\text{Si} + ^{63}\text{Cu}$  and  $^{28}\text{Si} + ^{74}\text{Ge}$  systems, respectively. Experimental fragment masses and energies were corrected for neutron evaporation and  $\gamma$ -ray emission, according to the procedure of Ref. 4.

For all the reactions investigated, the fragment TKE are almost independent of incident energy and observation angle. Furthermore, the TKE corresponding to symmetric mass division are in close agreement with the predictions of Viola's systematics<sup>20</sup> for fission processes. These features, generally found in the study of other fissionlike reactions in the medium-mass region, indicate that full relaxation of the kinetic energy of the composite system has occurred before scission time. To get further information on the system configuration at scission, the

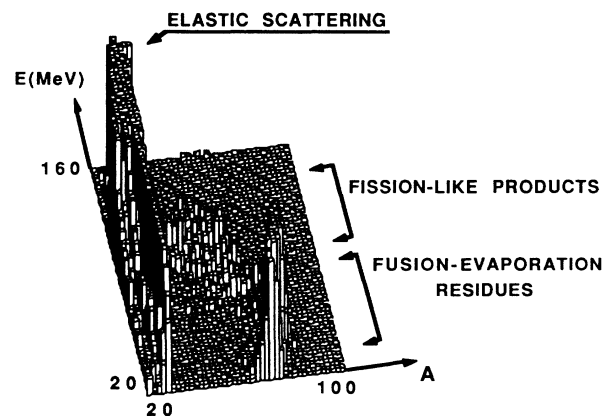


FIG. 2. Mass-energy spectrum for the  $^{28}\text{Si} + ^{63}\text{Cu}$  reaction at  $\theta_L = 20^\circ$  and  $E_i = 158$  MeV.

experimental TKE were compared to theoretical values calculated according to

$$\begin{aligned} \text{TKE} &= E_{\text{Coul}} + E_{\text{rot}} \\ &= Z_1 Z_2 e^2 / (R_1 + R_2 + d) \\ &\quad + [\hbar^2 l(l+1)] / [2\mu(R_1 + R_2 + d)^2], \end{aligned} \quad (3)$$

where  $R_1, R_2$  are the projectile and target nuclear radii,  $Z_1$  and  $Z_2$  the atomic numbers,  $l$  the exit-channel average angular momentum evaluated in the sticking limit,  $\mu$  the reduced mass, and  $d$  a distance parameter. This last quantity, accounting for the deformation of the composite system at scission (i.e., for departures from tangent-sphere configuration), was adjusted to reproduce the ex-

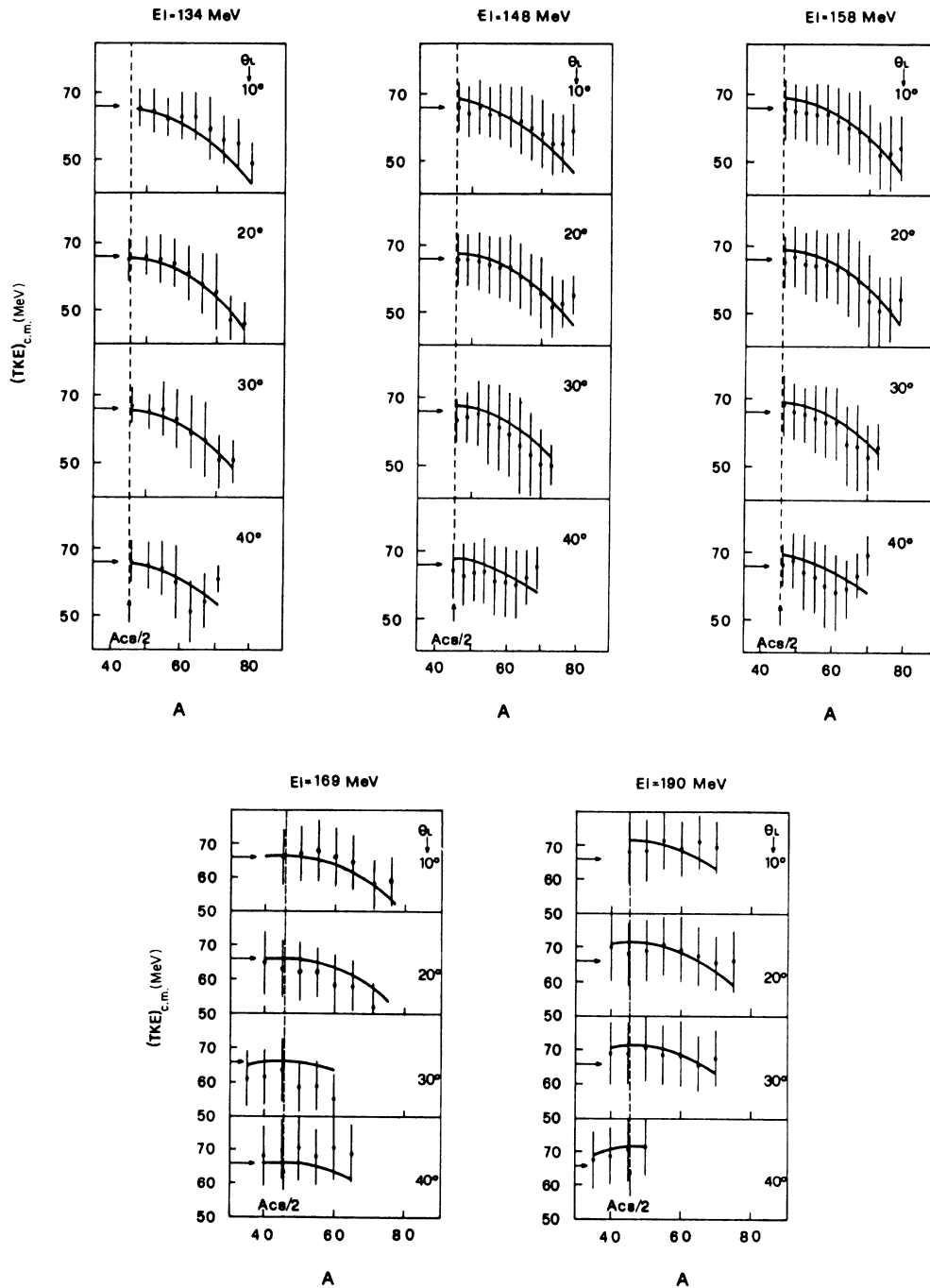


FIG. 3. Total kinetic energies of fissionlike fragments, as a function of fragment mass, for the  $^{28}\text{Si} + ^{63}\text{Cu}$  reaction (dots) and widths of the kinetic energy distributions (bars). Theoretical values, computed by use of Eq. (3), are displayed as solid lines. Predictions of the Viola's systematics for a fission process are indicated by arrows. Dashed lines correspond to half the composite system mass.

perimental TKE. The best-fit values were found to increase with incident energy so that the ratio  $(R_1 + R_2 + d)/(R_1 + R_2)$  varied from  $\approx 1.3$  to  $\approx 1.5$  for most of the systems investigated over the energy domain considered.

### B. Mass distributions of the fissionlike fragments

Center-of-mass double-differential cross sections  $(d^2\sigma/d\theta dA)_{c.m.}$  of the fissionlike events, as a function of fragment mass, are presented in Figs. 5–10 for the  $^{28}\text{Si} + ^{63}\text{Cu}$ ,  $^{35}\text{Cl} + ^{65}\text{Cu}$ ,  $^{37}\text{Cl} + ^{65}\text{Cu}$ ,  $^{28}\text{Si} + ^{74}\text{Ge}$ ,  $^{19}\text{F} + ^{89}\text{Y}$ ,  $^{28}\text{Si} + ^{89}\text{Y}$  reactions, respectively. For some incident energies and observation angles, the fragment mass spectra clearly exhibit memory of the entrance-channel mass asymmetry, showing pronounced peaks around the target mass. This indicates that in these cases no substantial mass drift occurred during the interaction time, as is frequently observed for fragment mass (or charge) distributions relative to DIC. However, a continuous evolution is seen with the observation angle. The mass spectra broaden progressively as the observation angle decreases, exhibiting shapes more symmetric around half the composite system mass. In general, this trend is more pronounced at lower incident energies, since for higher energies the cross section for symmetric splitting is approximately equal in magnitude to the targetlike production cross section. Such a behavior of the mass spectra is indicative of a mass asymmetry relaxation process and implies a characteristic time comparable to the rotation period of the composite system ( $\approx 10^{-21}$  s). A

remarkable exception to this trend is found for the  $^{32}\text{S} + ^{76}\text{Ge}$ ,  $^{28}\text{Si} + ^{89}\text{Y}$ , and  $^{19}\text{F} + ^{89}\text{Y}$  reactions. In the first reaction, no angle dependence was observed for the mass distributions, which exhibit maxima around half the composite system mass as in a fusion-fission process.<sup>4</sup> For the second and, to some extent, for the third system, which have the highest mass asymmetries considered in the present study, two distinct components are present in the mass distributions: an isotropic component, peaking at half the composite system mass, and an angle-dependent one, peaking at the target mass.

The evolution of the mass distributions with the total mass of the composite system appears in good agreement with the trend observed for the first time by Oeschler *et al.*,<sup>9</sup> namely narrow and symmetric (around  $A_{CS}/2$ ) distributions that broaden progressively as the system total mass decreases, peaking around the target mass in the case of the lightest systems.

### C. Angular distributions of the fissionlike fragments

As typical examples, c.m. double-differential cross sections  $(d^2\sigma/d\theta dA)_{c.m.}$ , as a function of  $\theta_{c.m.}$ , are reported in Figs. 11 and 12 for the  $^{28}\text{Si} + ^{63}\text{Cu}$  and  $^{28}\text{Si} + ^{74}\text{Ge}$  reactions, respectively. At lower incident energies, the cross sections tend to increase with the observation angle, a behavior which is more obvious for fragment masses close to the target mass. As the incident energy increases, the angular distributions are seen to flatten, in agreement with  $(d^2\sigma/d\theta dA)_{c.m.} = \text{const.}$ , as is observed in fission decay. However, this effect is somewhat at-

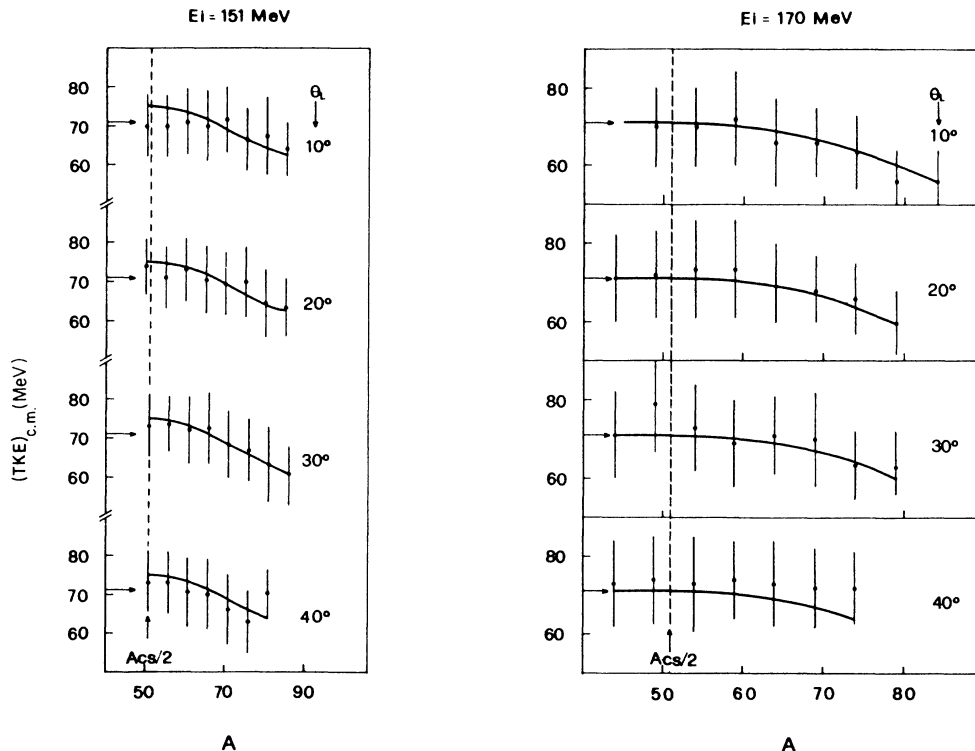


FIG. 4. Same as Fig. 3 for the  $^{28}\text{Si} + ^{74}\text{Ge}$  reaction.

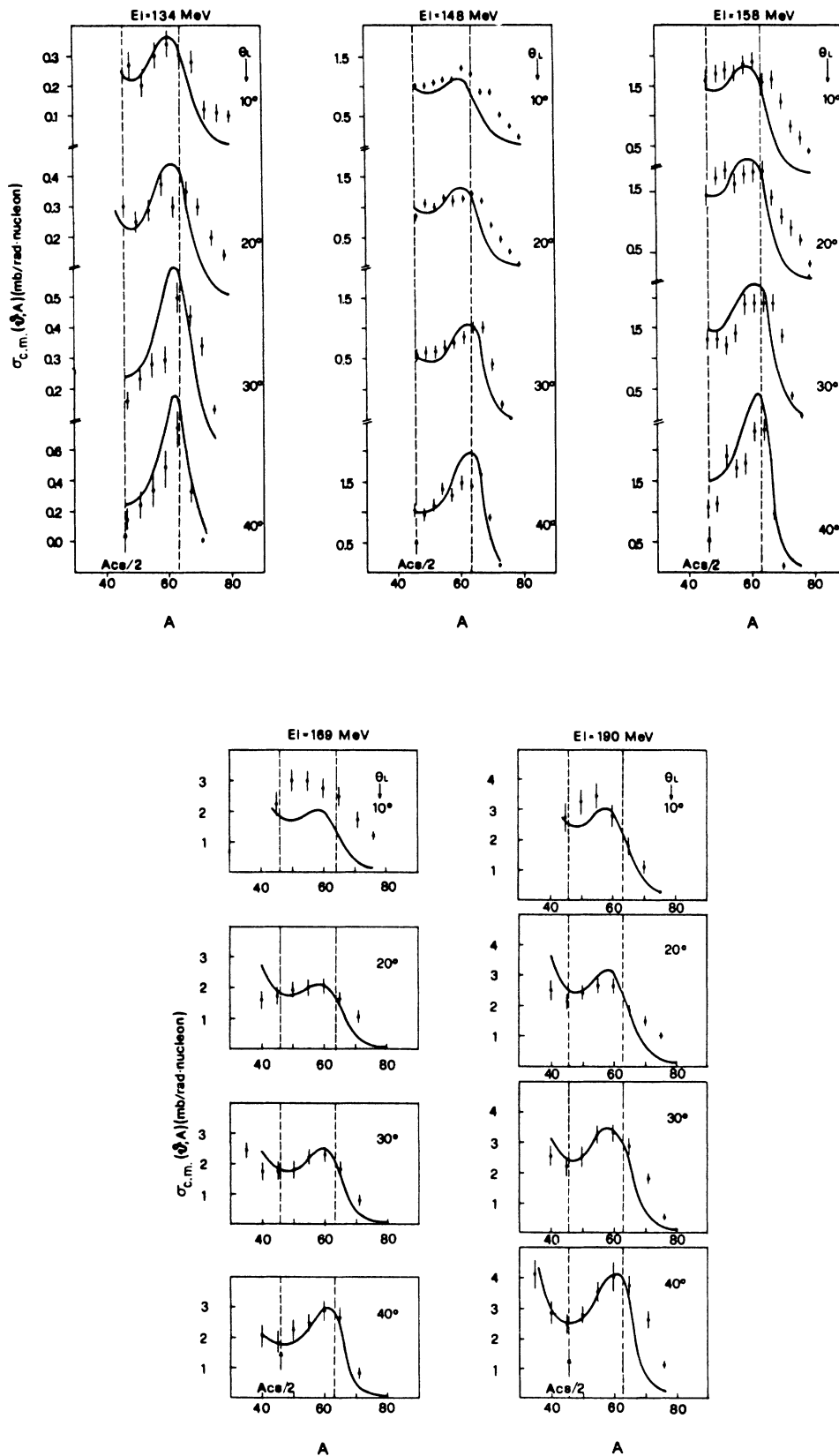


FIG. 5. Center-of-mass double-differential cross sections of the fissionlike events, as a function of the fragment mass, for the  $^{28}\text{Si} + ^{63}\text{Cu}$  reaction. Dashed lines correspond to half the composite system mass and to target mass. Solid lines are the predictions of the dynamical model described in Sec. IV A.

tenuated for the targetlike component, which still tends to increase with observation angle.

The characteristics of the fissionlike processes for the medium-mass systems investigated in the present study can be summarized as follows.

(i) For each composite system, the fragment mean kinetic energies are independent of the incident energy and observation angle. They can be reproduced by the sum of the Coulomb and the rotational energy. Moreover, the mean TKE corresponding to symmetric mass division are consistent with the predictions of Viola's systematics for fission processes.

(ii) The fragment mass distributions generally exhibit an evolution with the observation angle: from distributions peaking around the target mass (at large angles) to more symmetric (around  $A_{CS}/2$ ) shapes at forward angles.

(iii) The fragment angular distributions vary as a function of the fragment mass. They are generally compatible with a  $1/\sin\theta_{c.m.}$  behavior except for fragment masses close to the target mass, for which an increase with the observation angle is observed.

#### IV. DATA ANALYSIS AND DISCUSSION

The features of the fissionlike processes observed in the present study indicate that the necessary conditions for compound-nucleus (CN) fission (i) fully relaxed fragment energies, (ii) fragment mass distributions symmetric around  $A_{CS}/2$ , and (iii) fragment angular distributions proportional to  $1/\sin\theta_{c.m.}$  are only partially fulfilled by the present data.

The observation of asymmetric mass distributions could suggest the occurrence of an asymmetric fission process, if one considers that the fissility parameters of the lightest systems (see Table I) are very close to the Businaro-Gallone limit<sup>12</sup> ( $x_{BG}=0.4$ ). However, in this case one would expect no evolution of the mass distribution shapes with the observation angle, since the CN lifetime is much longer than the rotation periods of the composite systems considered. Furthermore, it must be noted that, according to the predictions of the rotating liquid-drop model (RLDM),<sup>13</sup> the Businaro-Gallone limit is expected to shift to lower values as the CN spin is increased. For CN spins  $\approx 60\hbar$  reached in the reactions of

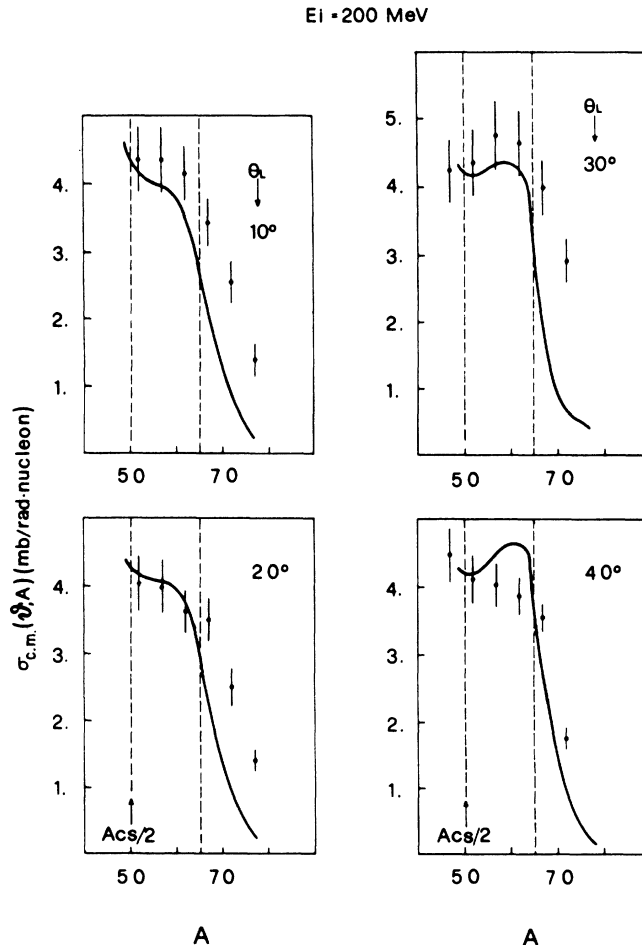


FIG. 6. Same as Fig. 5, for the  $^{35}\text{Cl} + ^{65}\text{Cu}$  reaction.

the present study, the RLDM yields  $x_{BG} \approx 0.3$ , a value which is out of the range of fissilities spanned in this work. As a consequence, the Businaro-Gallone limit cannot be an explanation for the present data.

Compound-nucleus formation implies that the intermediate system decays after having reached full statisti-

cal equilibrium in all of its degrees of freedom. In the present case, some degrees of freedom, like the kinetic energy, are fully equilibrated, while others like the mass asymmetry are not, as indicated by the evolution of the fragment mass and angular distributions. The mass asymmetry in particular is equilibrated in a time scale

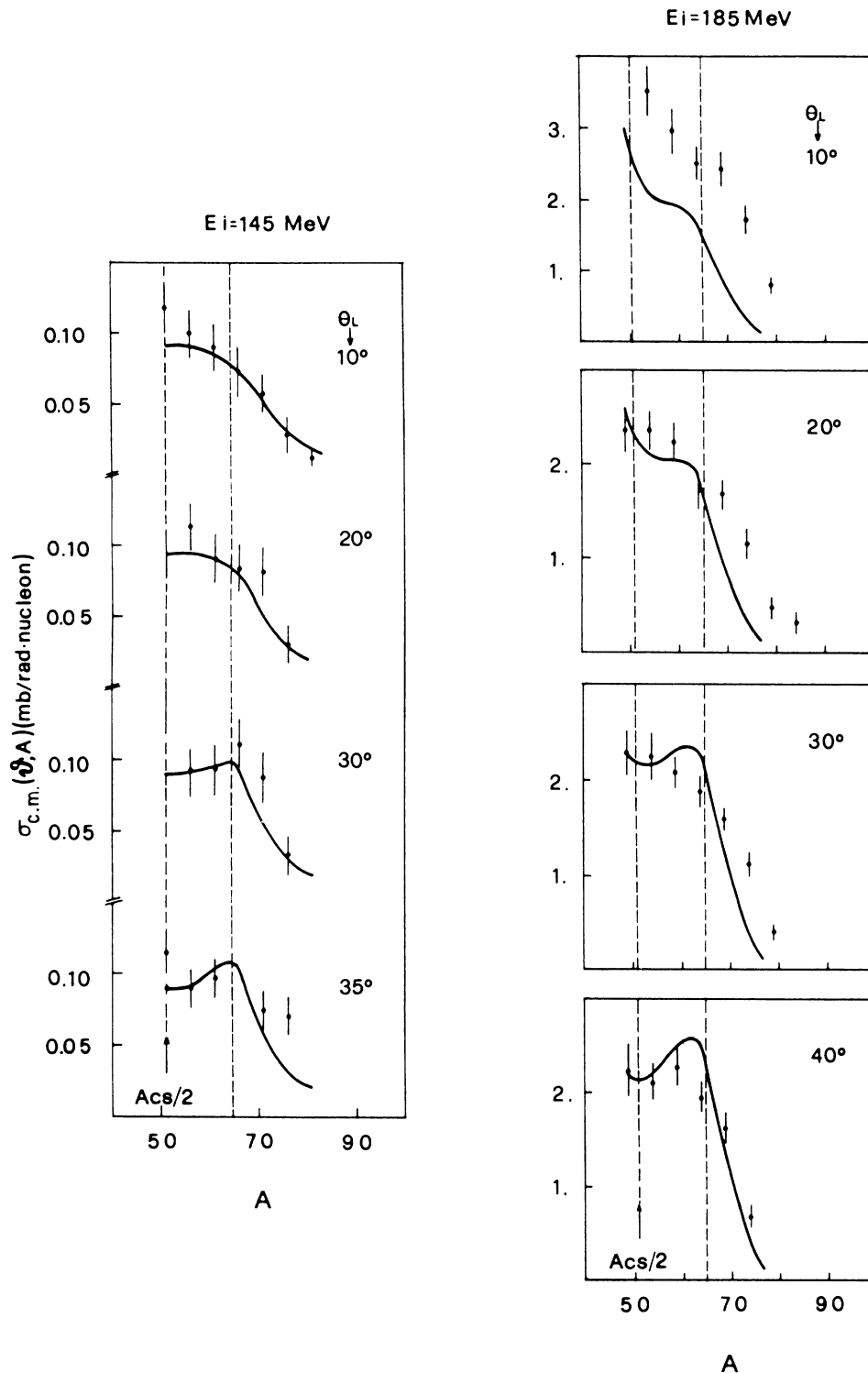
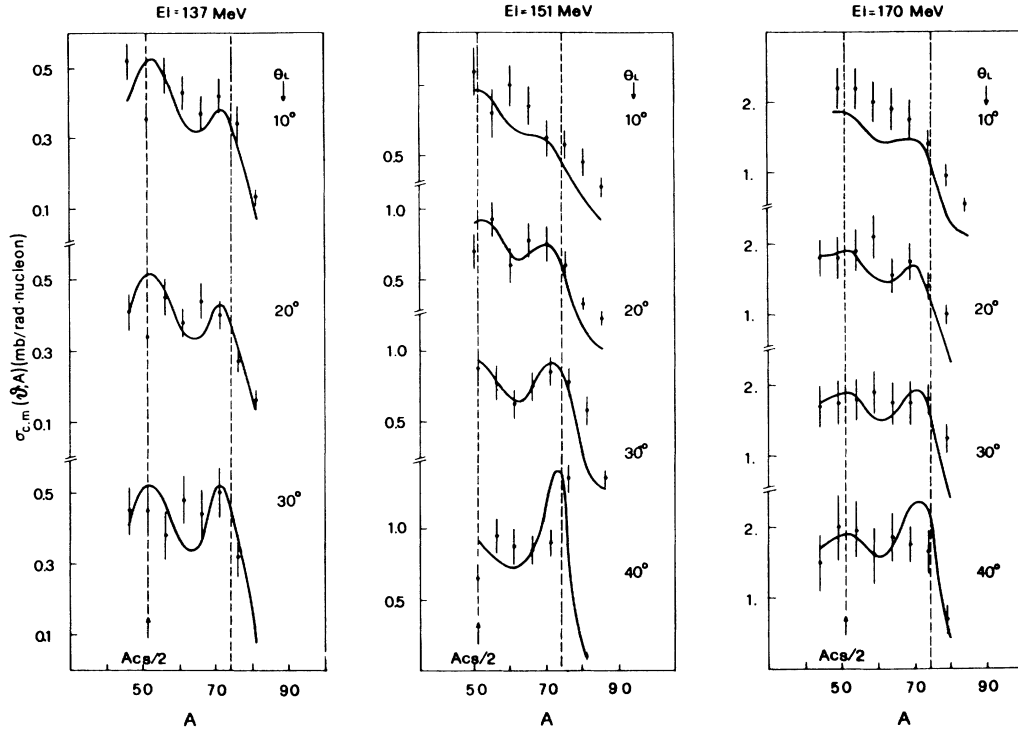


FIG. 7. Same as Fig. 5, for the  $^{37}\text{Cl} + ^{65}\text{Cu}$  reaction.

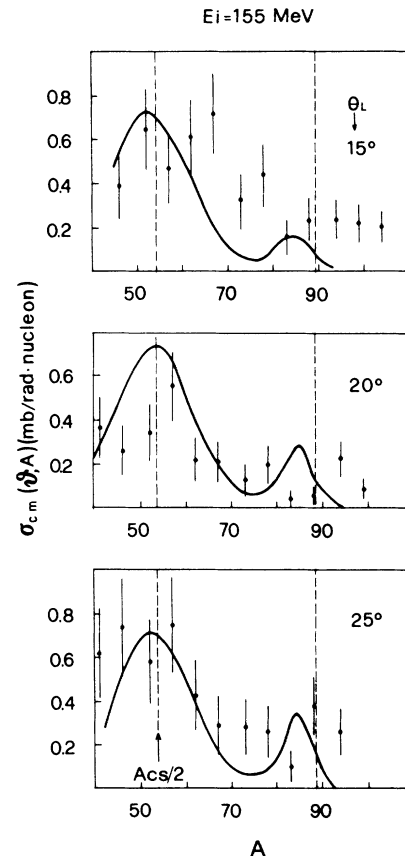


FIG. 8. Same as Fig. 5, for the  $^{28}\text{Si} + ^{74}\text{Ge}$  reaction.

comparable with the system rotation period. This implies that the mass distributions measured at different angles reflect different stages of the mass-asymmetry equilibration process.

The relaxation of the composite system proceeds faster along the energy coordinate than along the mass asymmetry coordinate, in close agreement with recent results on dissipative collisions.<sup>14</sup> According to the considerations of Sec. II A, the detection of fragments at very forward angles is expected to reflect later stages of the mass equilibration process. This is confirmed by the observation of fairly equilibrated mass distributions in the forward direction. The existence of long-lived and short-lived components in the fragment production cross section is also seen in the angular distributions. They are nearly flat for fragment masses not too close to the target mass, whereas the targetlike components tend to increase with observation angle. Such different behaviors can be understood by assuming that the targetlike fragments originate from earlier stages of the mass transfer process, while longer interaction times are required to bring the composite system to more symmetric configurations.

From the above considerations, it results that the fissionlike events presently studied originate from dissipative collisions in which the composite systems live long enough to allow most of the relevant degrees of freedom to be completely equilibrated, except for the mass asymmetry. This latter relaxes on a time scale comparable to the system rotation period. In this respect, both the reaction mechanism and the time scale appear intermediate with respect to the ones characterizing CN and DIC.

FIG. 9. Same as Fig. 5, for the  $^{19}\text{F} + ^{89}\text{Y}$  reaction.

### A. Data analysis with a dynamical model based on transport theory

As shown in previous studies,<sup>6,7</sup> transitional dissipative mechanisms are predicted, according to the fast-fission and extra-push models, to occur essentially in the heavy-mass region. We checked that, also in the present measurements, the necessary conditions for the above-mentioned models were not generally fulfilled. Therefore, following the procedure outlined in Ref. 6, data were ana-

lyzed with a dynamical model based on the transport theory. It is assumed that at the beginning of a nucleus-nucleus collision, a rotating dinuclear system is formed and undergoes progressive relaxation in its relevant degrees of freedom. According to the results of recent studies of dissipative collisions,<sup>14</sup> different characteristic times are associated with the relaxation of different degrees of freedom of the composite system. This means that, at the time of scission, the system may have reached full equilibrium only in some degrees of freedom (i.e., in those

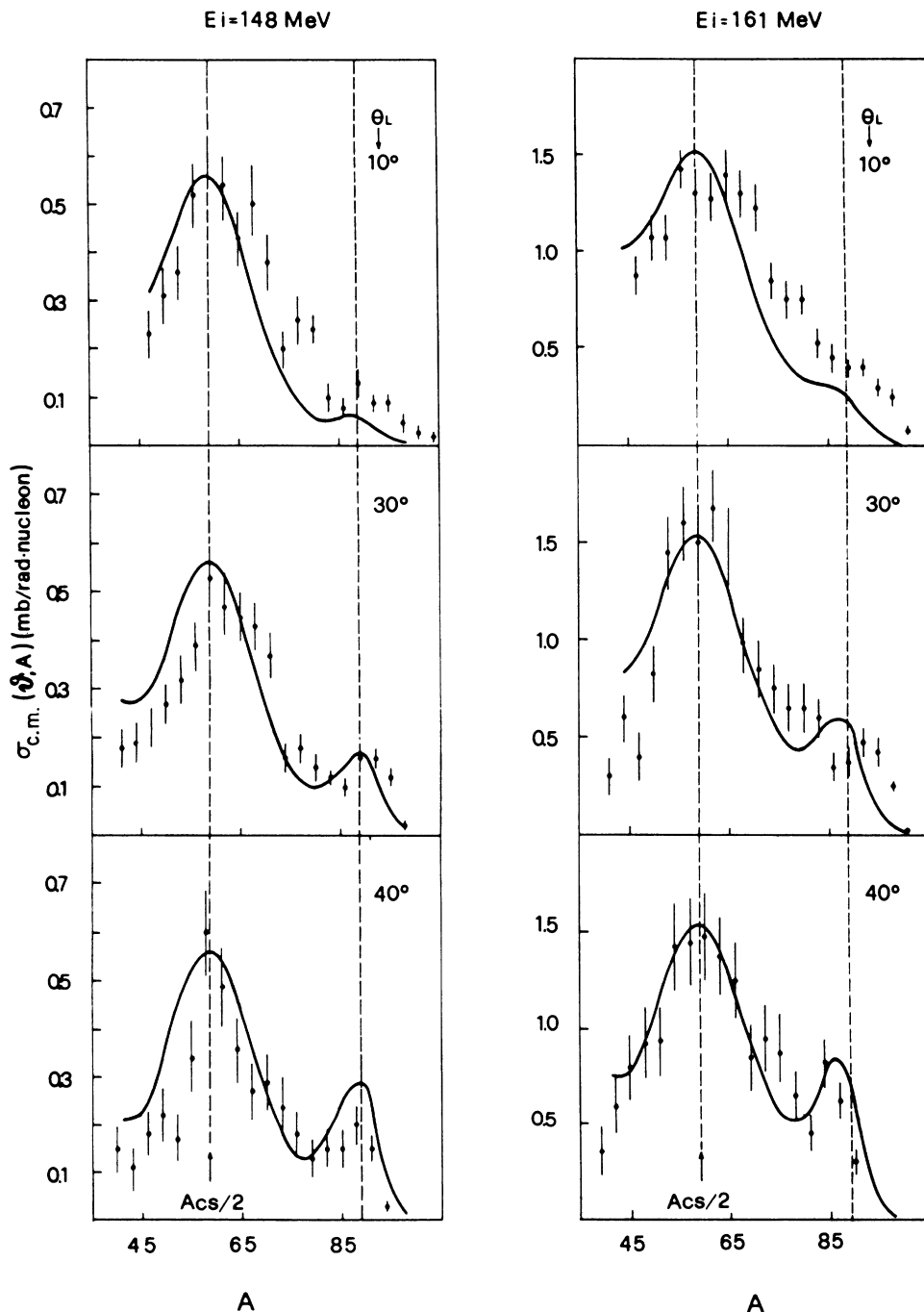


FIG. 10. Same as Fig. 5, for the  $^{28}\text{Si} + ^{89}\text{Y}$  reaction.

having shorter relaxation times). Relaxation is assumed to proceed by statistical nucleon exchange between the colliding nuclei during the system interaction time. The recent formulation of the transport theory by Nörenberg<sup>3</sup> is employed to evaluate the relaxation of the mass asymmetry attained by the system as a function of the interaction time. A statistical distribution of decay times is introduced according to Ref. 15, by stating that the probability of survival for the dinuclear system at a given time  $t$

is proportional to  $\exp(-t/\tau)$ , where  $\tau$  is the system lifetime. It is worth noting that  $\tau$  is the only free parameter in the present calculations, its value being adjusted (for each reaction) so that a *unique*  $\tau$  value is employed to reproduce *all the mass distributions* measured at a given incident energy. The relaxation of kinetic energy, angular momentum, and deformation degrees of freedom are evaluated by use of exponential functions of time, following Ref. 3. From the assumed probability distribution of

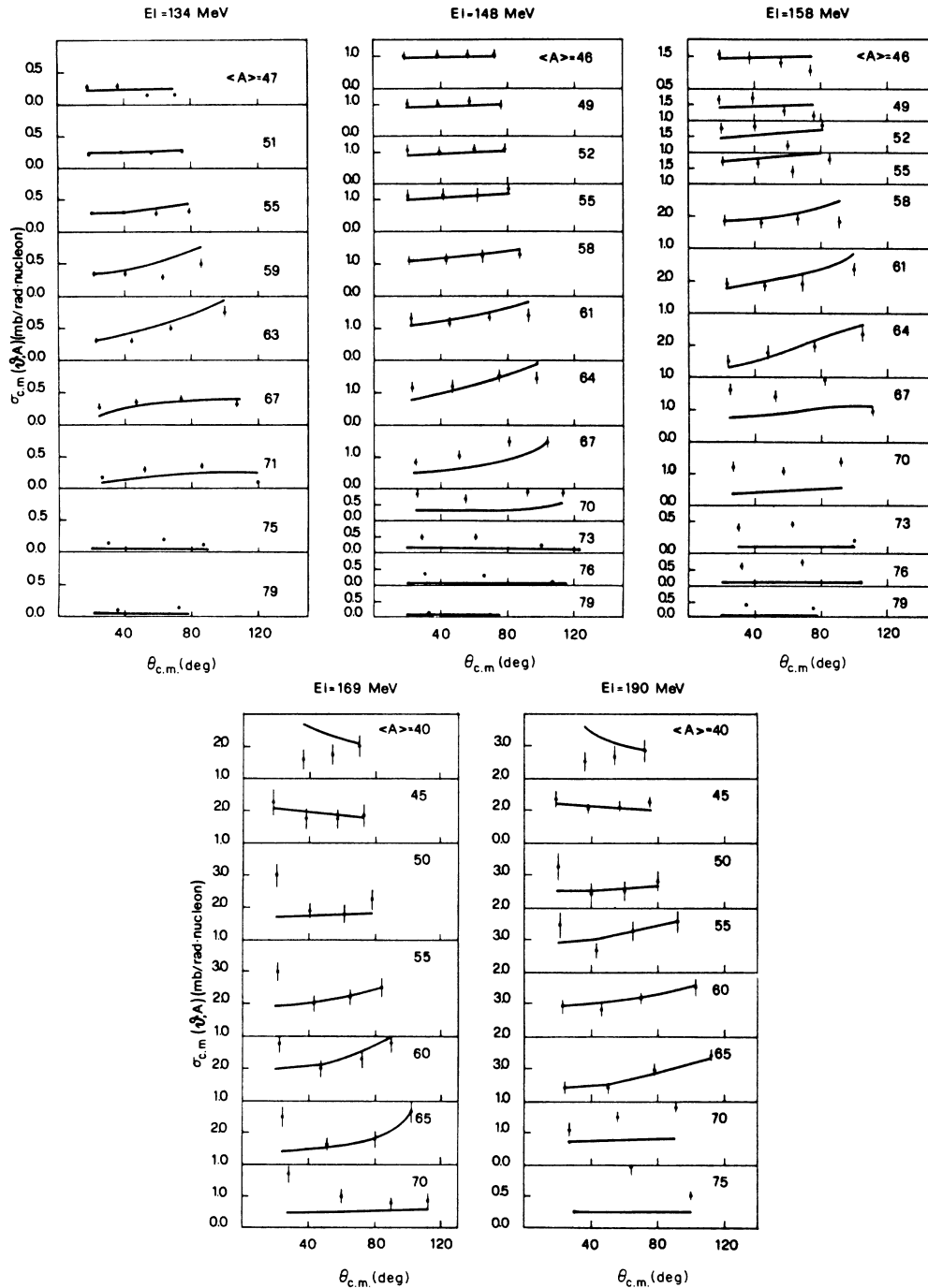


FIG. 11. Center-of-mass angular distributions of different masses ( $A$ ) of fissionlike fragments, for the  $^{28}\text{Si} + ^{63}\text{Cu}$  reaction. Solid lines are the predictions of the dynamical model described in Sec. IV A.

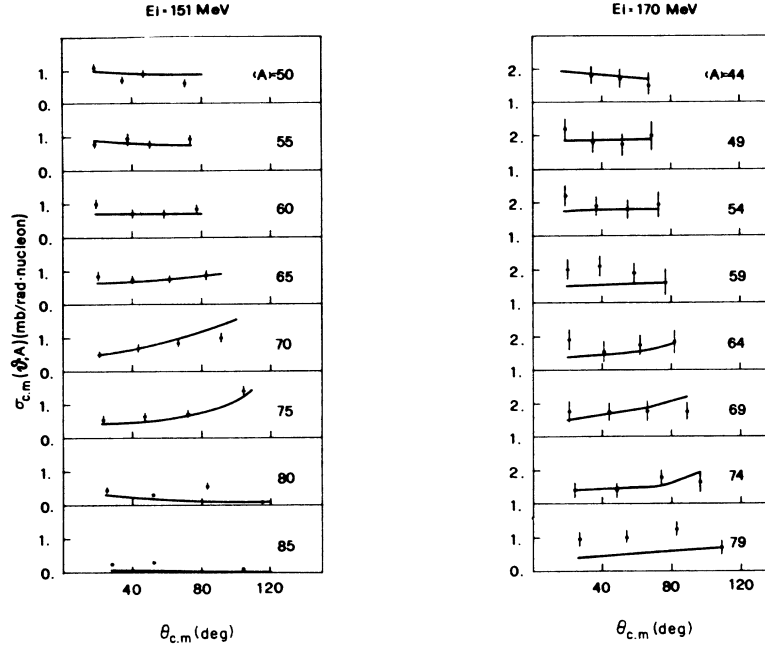


FIG. 12. Same as Fig. 11, for the  $^{28}\text{Si} + ^{74}\text{Ge}$  reaction.

decay times, the angular distribution of the fragments is computed by means of the angle-time correspondence

$$\Delta\theta = \int_0^{\Delta t} \omega(l, t) dt, \quad (4)$$

where  $\omega(l, t)$  is the angular velocity and  $l$  the angular momentum [see also Eq. (1)]. The time evolution of the mass asymmetry is computed by solving the Fokker-Planck equations for each involved partial wave in time steps of  $\approx 10^{-23}$  s. The resulting probability distributions for fragment masses are integrated over  $l$  in the  $l_{\text{cr}} \leq l \leq l_{\text{gr}}$  interval and then normalized on the basis of the corresponding “geometrical” reaction cross section. This latter is evaluated from the respective angular momentum interval, through a smooth cutoff approximation using Saxon-Woods functions, assuming for the critical ( $l_{\text{cr}}$ ) and the grazing ( $l_{\text{gr}}$ ) angular momenta their semiclassical estimates.<sup>16</sup> Besides this partially-equilibrated component ( $\sigma_{\text{PE}}$ ) of the fragment production cross section, the contribution of (angle-independent) fragmentation from a fully equilibrated system (i.e., for  $\tau \rightarrow \infty$ ) is computed. The cross section of this last process ( $\sigma_{\text{FE}}$ ) accounts for the existence of dynamical trajectories for which the system is trapped in a potential-energy barrier, i.e., for  $l_{\text{Bf=Bn}} \leq l \leq l_{\text{cr}}$  (the  $l$  values at which the fission barrier equals the neutron binding energy,  $l_{\text{Bf=Bn}}$ , have been taken from the RLDM estimates<sup>13</sup>). Details of the calculation procedure are given in Ref. 6. Results are presented in Figs. 5–12 (solid lines) for the reactions of the present study (for the  $^{32}\text{S} + ^{59}\text{Co}$  and  $^{32}\text{S} + ^{63}\text{Cu}$  reactions see Ref. 6; for  $^{32}\text{S} + ^{76}\text{Ge}$  see Ref. 7). The corresponding lifetime values, as well as the ratios  $\sigma_{\text{PE}}/(\sigma_{\text{PE}} + \sigma_{\text{FE}})$ , are reported in Table II. As can be realized by considering the magnitude of these ratios, almost 80% of the total fragment production cross section

is exhausted by nonfusion processes. This may explain why unreasonably low fission barriers have to be considered if one tries to reproduce such fissionlike data by statistical model calculations, assuming CN only as the fragment source.<sup>4</sup>

The experimental mass distributions are generally reproduced correctly both in shape and in absolute magnitude. This is true even for the cases where a noticeable evolution with angle or incident energy is observed. In particular, the expected mass drift is found to be correctly evaluated for all the systems studied. A further result is the ability of the present model to reproduce quantitatively the fragment mass and angular distributions originating from the decay of several nuclear systems spanning an ample range of mass asymmetry. Actually, experimental fragment charge (or mass) distributions for the  $^{12}\text{C} + ^{89}\text{Y}$ ,<sup>17</sup>  $^{12}\text{C} + ^{98}\text{Mo}$ ,<sup>17</sup>  $^{32}\text{S} + ^{50}\text{Ti}$ ,<sup>18</sup> and  $^{40}\text{Ca} + ^{64}\text{Ni}$  (Ref. 19) reactions were also correctly reproduced, and the extracted lifetimes have been included in Table II. The present analysis indicates that medium-mass composite systems, characterized by moderate asymmetry, have relatively long lifetimes (i.e., comparable to rotation periods) so that a substantial equilibration of the mass asymmetry can be observed. On the contrary, for very asymmetric systems, the short lifetime sets a limit on the attainable equilibration of the mass asymmetry. This yields fragment mass (charge) distributions which normally exhibit two distinct components, namely projectilelike (targetlike), and fusion-fission-like components, both having angle-independent centroids.

### B. Lifetime systematics

The general trend of lifetime, as a function of both the c.m. energy and the mass asymmetry, for the composite

systems of the present study, is displayed in the tridimensional plot of Fig. 13. Lifetimes appear to increase with  $E_{c.m.}$ , while they drop by an order of magnitude as the mass asymmetry varies from  $\approx 0.2$  to  $\approx 0.8$ . The  $\tau$  dependence on the incident energy suggests that the mass equilibration rate is determined by the amount of kinetic energy and of angular momentum dissipated. This can be expected if one considers, in particular, the expression of the mass-drift coefficient<sup>3</sup> adopted in the present analysis, which depends explicitly on the excitation energy and the angular momentum of the system.

Due to the lifetime dependence on the incident energy, any trend which can be found for lifetimes as a function of the composite system mass and mass asymmetry is obviously biased by the choice of the particular incident energies considered. Nevertheless, unbiased information can be acquired provided that data are analyzed in a suitable energy-independent representation. Among the pos-

sible choices, the simple scaling  $f(\tau)=\tau/l_{gr}$  was considered because of its effectiveness. As can be realized from the data in Table II, for each composite system the reduced  $\tau$  values are scattered around a mean value, with a rms deviation of typically  $\approx 10\%$  of the mean value. Moreover, there is no obvious monotonic dependence of  $\tau/l_{gr}$  on  $E_{c.m.}$  throughout the investigated range.

The reduced lifetimes are displayed as a function of mass asymmetry in Fig. 14 for the reactions listed in Table II. In this figure both the mean value and the rms deviation of the  $\tau/l_{gr}$  distributions are reported (a rms deviation of 20% of the mean value was estimated for data taken at only one incident energy). The reduced lifetimes are seen to decrease in quite a linear fashion as the mass asymmetry increases. The large amount of data exhibiting the present tendency indicates this as a “universal” feature of the transitional dissipative mechanisms. Reduced lifetimes of Table II were least-squares fitted to

TABLE II. Results of data analysis performed with the dynamical model described in Sec. IV A: the lifetime ( $\tau$ ), the reduced lifetime ( $\tau/l_{gr}$ ) and the ratio between the partially ( $\sigma_{PE}$ ) and the partially plus the fully equilibrated ( $\sigma_{PE}+\sigma_{FE}$ ) components of the theoretical fragment production cross section are reported for each reaction and incident energy.

Reaction	$E_i$ (MeV)	$\tau$ ( $10^{-22}$ s)	$\tau/l_{gr}$ ( $10^{-22}$ s)	$\sigma_{PE}/(\sigma_{PE}+\sigma_{FE})$	Ref.
$^{32}\text{S} + ^{50}\text{Ti}$	131	7.9	0.141	1.00	18
	166	12.3	0.171	0.97	18
$^{32}\text{S} + ^{59}\text{Co}$	126	6.3	0.123	1.00	6
	140	6.9	0.115	1.00	6
	154	11.5	0.171	1.00	6
	168	12.3	0.165	0.87	6
$^{28}\text{Si} + ^{63}\text{Cu}$	134	7.6	0.123	0.98	<sup>a</sup>
	148	9.4	0.136	0.93	<sup>a</sup>
	158	10.9	0.149	0.93	<sup>a</sup>
	169	9.2	0.118	0.89	<sup>a</sup>
	190	9.8	0.113	0.83	<sup>a</sup>
$^{32}\text{S} + ^{63}\text{Cu}$	126	7.2	0.142	1.00	6
	140	7.6	0.128	1.00	6
	154	10.2	0.151	0.94	6
	168	11.4	0.152	0.93	6
$^{35}\text{Cl} + ^{65}\text{Cu}$	200	13.7	0.153	0.80	<sup>a</sup>
$^{12}\text{C} + ^{89}\text{Y}$	197	0.94	0.011	0.99	17
$^{37}\text{Cl} + ^{65}\text{Cu}$	145	9.4	0.146	0.55	<sup>a</sup>
	185	10.8	0.130	0.87	<sup>a</sup>
$^{28}\text{Si} + ^{74}\text{Ge}$	137	7.2	0.108	0.86	<sup>a</sup>
	151	7.2	0.097	0.86	<sup>a</sup>
	170	9.4	0.112	0.85	<sup>a</sup>
$^{40}\text{Ca} + ^{64}\text{Ni}$	182	12.3	0.166	0.91	19
$^{32}\text{S} + ^{76}\text{Ge}$	218	14.4	0.139	0.78	4
$^{19}\text{F} + ^{89}\text{Y}$	155	2.7	0.034	0.94	<sup>a</sup>
$^{12}\text{C} + ^{98}\text{Mo}$	107	0.86	0.015	1.00	17
	197	1.1	0.013	0.99	17
$^{28}\text{Si} + ^{89}\text{Y}$	148	5.3	0.074	0.90	<sup>a</sup>
	161	6.8	0.085	0.80	<sup>a</sup>

<sup>a</sup>Present work.

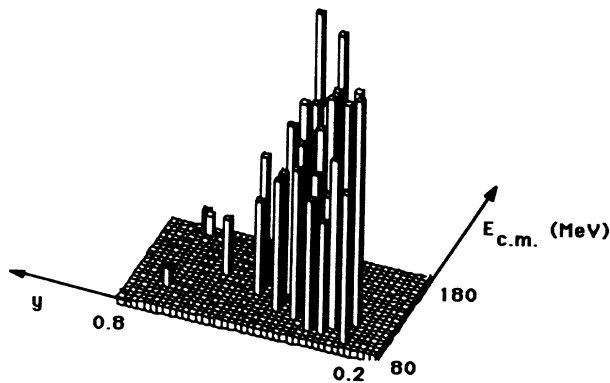


FIG. 13. Mass asymmetry-energy scatter plot of lifetime values obtained from data analysis with the dynamical model described in Sec. IV A.

polynomial functions of  $y$ . The normalized chi square was found to be minimized ( $\chi^2/n=1.09$ ) by the linear function  $\tau/l_{gr}=0.224-0.276y$ .

In the case of very asymmetric systems ( $y \approx 0.8$ ) however,  $\tau$  values tend to level off around a constant value which is comparable to the characteristic time for kinetic energy dissipation ( $t_E=3 \times 10^{-22}$  s).<sup>3</sup> This departure, confirmed also for the  $^{12}\text{C} + ^{116}\text{Sn}$  (Ref. 17) system lifetime (not reported in Fig. 14), can be understood considering that the observation of fully relaxed fragment kinetic energies in such reactions<sup>17</sup> implies  $\tau \geq t_E$ , i.e., a lower limit for  $\tau$ . As further evidence, mass asymmetry equilibration in such reactions is not observed as one would expect if the lifetimes of these very asymmetric systems were 1 order of magnitude shorter than the characteristic time of the mass equilibration process.

The dependence of lifetime on the system total mass is displayed in Fig. 15. For composite system masses  $A_{CS} \leq 100$ , reduced lifetimes are seen to be nearly constant within the quoted uncertainties. As  $A_{CS}$  increases beyond 100, however, this constancy is broken, the  $\tau/l_{gr}$  values varying even by factors approximately equal to 3–10. Such variations are also observed for different reactions leading to a given composite system (see, for example, the  $A_{CS}=102$  and 108 systems). Since in these cases the major difference relates to the entrance-channel characteristics, this reinforces the indication of the fundamental role of the mass asymmetry in these reaction mechanisms. Such an indication, on the other hand, has also a correspondence in the basic assumptions of dynamical models like the “fast fission” and the “extra push.” In the former, the mass asymmetry is explicitly introduced as a coordinate of the collective configuration space, containing the bulk of the information on the reaction. In the latter, the reaction dynamics is modeled on the geometry of the nuclear configuration, which takes into account the mass asymmetry.

## V. SUMMARY AND CONCLUSION

The results of a systematic experimental investigation of the fissionlike processes for medium-mass nuclear systems have been presented. Mass, angular, and kinetic energy distributions of fragments were measured for ten reactions, at incident energies in the  $E/A=(4-7)$  MeV/nucleon range and observation angles  $\theta_L=5^\circ-40^\circ$ . To study the dependence of the reaction mechanism on the entrance-channel mass asymmetry, various projectile-target combinations and incident energies were chosen to form the same composite systems at comparable angular momenta. The relaxation of the mass asym-

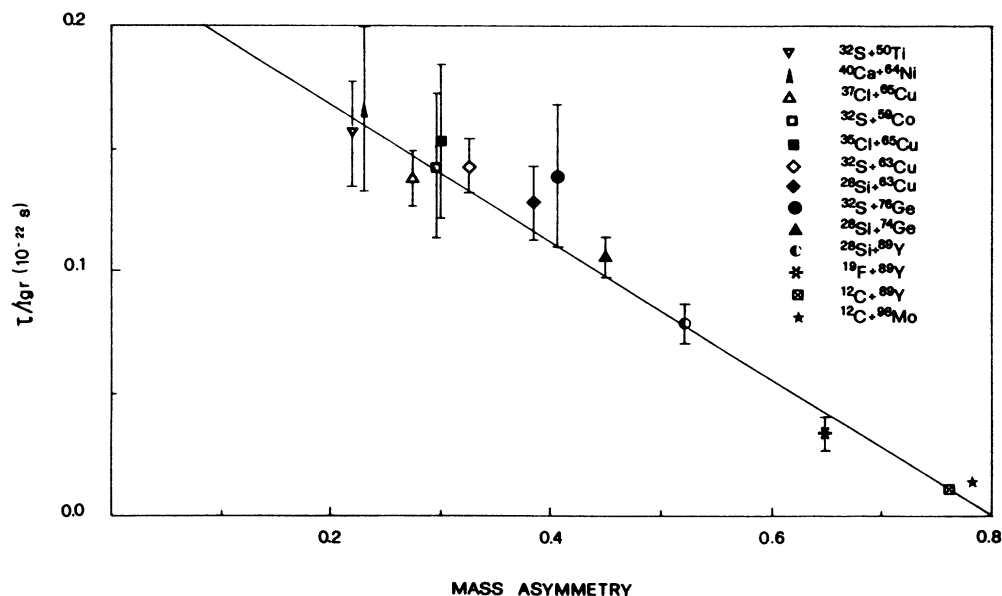


FIG. 14. Plot of reduced lifetimes, as a function of the mass asymmetry ( $y$ ), for the reactions of Table II. Solid line shows the result of a best-fit analysis with polynomial functions of  $y$ .

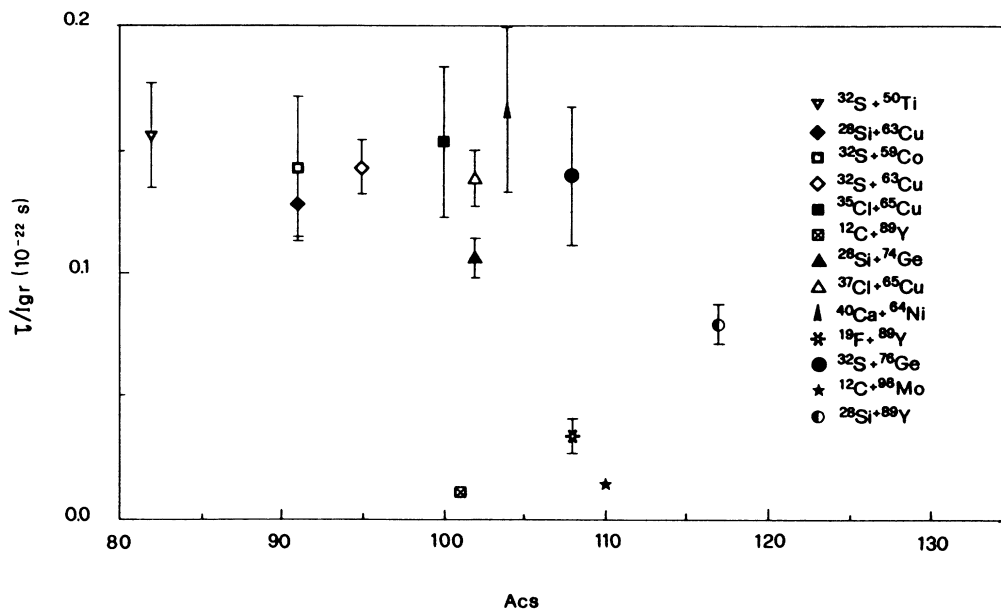


FIG. 15. Plot of reduced lifetimes, as a function of the composite system mass ( $A_{CS}$ ), for the reactions of Table II.

metry degree of freedom is observed as an evolution of the mass spectra: they vary from distributions peaking around the target mass, to more symmetric shapes peaking around half the composite system mass. The fragment angular distributions are generally compatible with a  $1/\sin\theta_{c.m.}$  behavior. The fragment mean total kinetic energies are fully relaxed and consistent with the predictions of Viola's systematics for symmetric fission. The observed features cannot be interpreted in terms of deep inelastic or fusion-fission processes. They indicate that the mass asymmetry degree of freedom evolves towards equilibration, after the kinetic energy has been fully dissipated, on a time scale comparable to the system rotation period. The characteristics of such processes, as well as the time scale, indicate the existence of a transitional dissipative mechanism of an intermediate type with respect to deep inelastic reactions and fusion-fission.

The experimental double-differential cross sections are correctly reproduced both in shape and in absolute value by the present dynamical-model calculations based on the recent formulation of the transport theory by Nörenberg. Lifetimes of the composite systems studied in the present work have been determined by comparing calculated to experimental double-differential cross sections.

Systematics of lifetimes obtained in the present study are presented and discussed. For a given system, the lifetime is found to increase with the incident energy, indicating that the mass equilibration rate is determined by

the amount of kinetic energy and angular momentum dissipated. The lifetime expressed in units of the grazing angular momentum exhibits a linear decrease as the composite-system mass asymmetry increases, showing a universal trend for the transitional mechanisms investigated. No significant trend is found for the lifetime as a function of the composite-system mass.

A general result of the present analysis is the possibility of describing the reaction mechanisms of dissipative collisions for different medium-mass systems exhibiting various phenomenologies. Such mechanisms are described in terms of a continuous relaxation process, leading the composite system from the entrance channel to more or less equilibrated configurations, depending on the system lifetime. At the extremes of this general evolution process, i.e., in the limit of very short or long lifetimes, deep-inelastic reactions and fusion-fission are found, respectively, as characteristic processes exhibiting the equilibration in only some, or in all, of the relevant degrees of freedom.

In conclusion, the present data allow a detailed understanding of the reaction mechanisms in the medium-mass region at low incident energy. They help to summarize and correlate the bulk of existing data relative to these systems with theoretical descriptions, and suggest new theoretical developments by pointing out still open questions.

<sup>1</sup>C. Grégoire, C. Ngo, and E. Tomasi, Proceedings of the International Conference on Selected Aspects of Heavy Ion Reactions, Saclay, 1982, edited by Commissariat à l'Énergie Atomique (unpublished); Nucl. Phys. **A387**, 37c (1982).

<sup>2</sup>W. J. Swiatecki, Phys. Scr. **24**, 113 (1981); S. Bjornholm and W. J. Swiatecki, Nucl. Phys. **A391**, 471 (1982).

<sup>3</sup>See A. Gobbi and W. Nörenberg, in *Heavy Ion Collisions*, edited by R. Bock (North-Holland, Amsterdam, 1980), Vol. 2, pp.

- 128–273, and references therein.
- <sup>4</sup>G. Guillaume, J. P. Coffin, F. Rami, P. Engelstein, B. Heusch, P. Wagner, P. Fintz, J. Barrette, and H. E. Wegner, *Phys. Rev. C* **26**, 2458 (1982).
- <sup>5</sup>J. P. Coffin, G. Guillaume, A. Fahli, F. Rami, B. Heusch, P. Wagner, P. Engelstein, P. Fintz, and N. Cindro, *Phys. Rev. C* **30**, 539 (1984).
- <sup>6</sup>S. Agnoli, I. Massa, G. Vannini, P. Boccaccio, F. Reffo, L. Vannucci, I. Iori, and R. A. Ricci, *Nucl. Phys.* **A464**, 103 (1987).
- <sup>7</sup>M. Gentili, I. Massa, G. Vannini, P. Boccaccio, F. Reffo, L. Vannucci, R. A. Ricci, and I. Iori, *Lett. Nuovo Cimento* **40**, 505 (1984).
- <sup>8</sup>M. Gentili, I. Massa, G. Vannini, P. Boccaccio, F. Reffo, L. Vannucci, R. A. Ricci, and I. Iori, *Lett. Nuovo Cimento* **39**, 205 (1984).
- <sup>9</sup>H. Oeschler, P. Wagner, J. P. Coffin, P. Engelstein, and B. Heusch, *Phys. Lett.* **87B**, 193 (1979).
- <sup>10</sup>J. R. Nix, *Nucl. Phys.* **A130**, 241 (1969).
- <sup>11</sup>C. K. Gelbke, P. Braun-Munzinger, J. Barrette, B. Zeidman, M. J. Levine, A. Gamp, H. L. Harney, and Th. Walcher, *Nucl. Phys.* **A269**, 460 (1976).
- <sup>12</sup>U. L. Businaro and S. Gallone, *Nuovo Cimento* **1**, 629 (1955); **1**, 1277 (1955).
- <sup>13</sup>S. Cohen, F. Plasil and W. J. Swiatecki, *Ann. Phys.* **82**, 557 (1974).
- <sup>14</sup>See, for example, H. Freiesleben and J. V. Kratz, *Phys. Rep.* **106**, 1 (1984), and references therein.
- <sup>15</sup>S. Agarwal, *Z. Phys.* **A297**, 41 (1980).
- <sup>16</sup>R. Bass, *Nuclear Reactions with Heavy Ions* (Springer, Berlin, 1980).
- <sup>17</sup>J. B. Natowitz, M. N. Namboodiri, and E. T. Chulick, *Phys. Rev. C* **13**, 171 (1976).
- <sup>18</sup>J. Barrette, P. Braun-Munzinger, C. K. Gelbke, H. E. Wegner, B. Zeidman, A. Gamp, H. L. Harney, and Th. Walcher, *Nucl. Phys.* **A279**, 125 (1977).
- <sup>19</sup>S. Agarwal, J. Galin, B. Gatty, D. Guerreau, M. Lefort, X. Tarrago, R. Babinet, B. Cauvin, J. Girard, and H. Nifenecker, *Nucl. Phys.* **A293**, 230 (1977).
- <sup>20</sup>V. E. Viola, Jr., *Nucl. Data Sheets* **A1**, 391 (1966).